CrossMark

# Thermomagnetometric analysis of lithium ferrites

Alexander Astafyev[1] · Elena Lysenko[1] · Anatoliy Surzhikov[1]

## Abstract

In this work, the magneto-phase transitions in pure lithium ($Li_{0.5}Fe_{2.5}O_4$), lithium–zinc ($Li_{0.4}Fe_{2.4}Zn_{0.2}O_4$) and lithium–titanium ($Li_{0.6}Fe_{2.2}Ti_{0.2}O_4$) ferrites were studied by the thermogravimetric analysis in magnetic field, which is known as the thermomagnetometry method. The ferrites were prepared by the solid-state synthesis from oxides and carbonates. The Curie point of magnetic phase in ferrites and their composite mixtures was determined from the derivative thermogravimetric curve in the region of ferrite mass change associated with the ferrimagnet–paramagnet transition in the magnetic phase. The method based on the analysis of ferrite mass change at Curie temperature was developed to estimate the ferrite phase concentrations in composite magnetic materials.

**Keywords** Lithium ferrite · LiZn ferrite · LiTi ferrite · Thermogravimetry · Thermomagnetometry · Curie temperature

## Introduction

The problem of estimating the phase composition of multicomponent magnetic materials including ferrites because of the impossibility of correct decomposition of X-ray reflections from phases with similar lattice parameters in this kind of materials leads to the necessity of developing the additional methods for controlling the phase composition [1, 2]. One of these methods is thermomagnetometric (TM) analysis based on thermogravimetric (TG) measurements in a magnetic field [3, 4].

As was known [5], when a ferro- or ferrimagnetic material is heated in a magnetic field at thermogravimetric measurements, a change in the mass of the sample is observed on the TG curve (increase or decrease in the mass depending upon the direction of the magnetic field gradient) in the region of the magneto-phase transition, which determines the temperature of the transition from the

magnetic state to the paramagnetic state of the material. So, it is possible to determine the Curie temperature of the sample with a sufficiently high accuracy by the derivative TG (DTG) curve.

Once the Curie temperatures have been accurately determined for a series of materials, then that information can be used to identify unknown samples or materials of known Curie temperature [6] and can be used for calibration of the temperature in the sample [7, 8]. The qualitative analysis connects to the relatively simple fast measurement and its ability to distinguish between various substituted ferrites or garnets, whose X-ray diffraction patterns can be very similar. As given in [1], the lattice parameters for $Li_{0.5(1+x)}Fe_{2.5-1.5x}Ti_xO_4$ ferrite at $x = 0$ and 0.6 were 8.330 and 8.348 Å, respectively. For the same $x$ values, the Curie points were observed at 630 and 300 °C. Thus, the relative change in the lattice parameter was $\sim 0.2\%$, whereas the relative displacement of the DTG temperature peak was 52%.

A tutorial review and the references therein describe TM and some of its applications [9]. The potentialities of TM method have been shown in a number of works that have focused on metals [10], ferromagnetic metallic glasses [11] and rare-earth iron garnets [12]. In our previous works [1, 13], it was found that TM analysis allows defining the temperature of the magnetic phase transitions in substituted lithium ferrites more precisely; consequently, it can more fully characterize the phase composition of a sample.

✉ Elena Lysenko
lysenkoen@tpu.ru

Alexander Astafyev
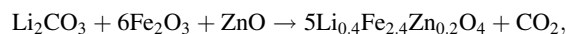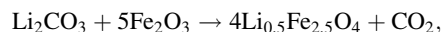astafeval@tpu.ru

Anatoliy Surzhikov
surzhikov@tpu.ru

[1] Tomsk Polytechnic University, 30, Lenin Avenue, Tomsk, Russia 634050

However, a complex analysis using both X-ray and TM methods will be the most optimal in case of the non-magnetic formation or weakly magnetic phase.

In the present work, the method of quantitative ferrite phase control based on TM analysis of the pure and substituted by zinc and titanium lithium ferrites was developed and tested using the samples with various concentrations of these ferrites.

## Experimental

The pure lithium ferrite (LiF), substituted lithium–zinc (LiZnF) and lithium–titanium (LiTiF) ferrites were prepared by the solid-state synthesis from commercial $Fe_2O_3$, $Li_2CO_3$, $ZnO$ and $TiO_2$ powders in accordance with the following reactions:

$Li_2CO_3 + 5Fe_2O_3 \rightarrow 4Li_{0.5}Fe_{2.5}O_4 + CO_2,$

$Li_2CO_3 + 6Fe_2O_3 + ZnO \rightarrow 5Li_{0.4}Fe_{2.4}Zn_{0.2}O_4 + CO_2,$

$0.6Li_2CO_3 + 2.2Fe_2O_3 + 0.4TiO_2 \rightarrow 2Li_{0.6}Fe_{2.2}Ti_{0.2}O_4 + CO_2.$

The synthesis including intermediate grinding and mixing of ferrite powders was performed in air at 800 °C and 360 min using a resistance furnace.

The synthesized ferrites were examined by X-ray diffraction (XRD) analysis that was carried out using ARL X'TRA diffractometer (CuKα radiation). XRD patterns were recorded in the $2\theta$ range 10°–70° with the scanning rate of $0.02°\ s^{-1}$ and then were processed by the full-profile analysis using a Powder Cell 2.5 software. The phases were identified by comparing the peaks with those presented in the PDF-4+ powder database of the International Center for Diffraction Data.

XRD patterns showed that the crystal structure of synthesized ferrites is a single-phase spinel with the lattice parameters of 0.8330 nm for Li ferrite, 0.8364 nm for LiZn ferrite and 0.8335 nm for LiTi ferrite, which are in good agreement with the literature data.

The saturation magnetization ($M_s$) of ferrites was measured at room temperature using a vibrating sample magnetometer with the maximum field of 10 kOe.

The thermomagnetometric analysis was performed in air using a STA 449C Jupiter thermal analyzer (Netzsch-Gerätebau GmbH). A part of the equipment including a heating furnace, a sample holder, and thermocouple is schematically shown in Fig. 1. The sample, consisting of ferrite or composite mixture from ferrites, with a mass of 30 mg was placed in the alumina crucible and was heated up to 700 °C in air with a heating rate of 50 °C min$^{-1}$. To control magnetic properties of ferrite sample, assembly of two small permanent magnets creating a field of $\sim$ 5 Oe was attached on the outer side of the furnace. The magnets
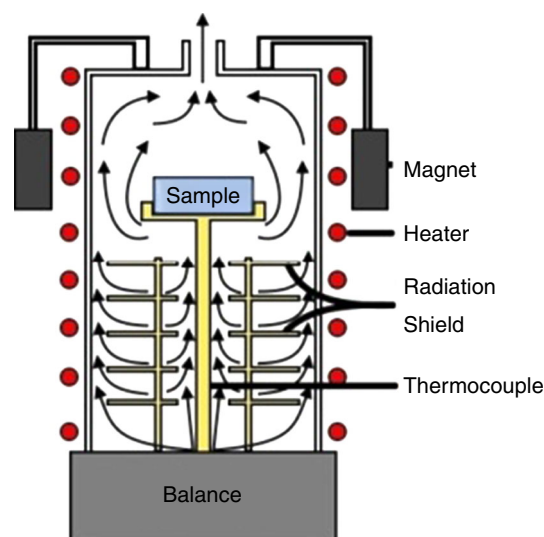


**Fig. 1** Block measuring system in thermal analyzer

were placed slightly above the sample; such geometric arrangement leads to the sample retraction into the external magnetic field and thus the measured mass of this sample changes. The Netzsch Proteus Analysis software was used for TG data analysis.

## Results and discussion

It is known that the lithium ferrite adopts an inverse spinel structure of the general formula $AB_2O_4$ in which the $Li^+$ ions and three-fifth of the $Fe^{3+}$ ions occupy the octahedral B-sites while the remaining $Fe^{3+}$ ions occupy tetrahedral A-sites [14]. The magnetic properties of $Li_{0.5}Fe_{2.5}O_4$ can be modified by substituting magnetic and/or diamagnetic cations for $Fe^{3+}$ ions on either sublattice [15–17]. Thus, the substitution in $Li_{0.5}Fe_{2.5}O_4$ ferrite by $Zn^{2+}$ ions increases the saturation magnetization of $Li_{0.5(1-x)}Fe_{2.5-0.5x}Zn_xO_4$ ferrite; however, a decrease in $M_s$ occurs with increasing $Zn^{2+}$ content above 0.4 [18, 19]. On the contrary, the $Ti^{4+}$ introduction in the lithium ferrite leads to decrease in $M_s$ [20, 21]. The saturation magnetizations for investigated ferrites were measured to be 55, 72 and 47 emu g$^{-1}$ for LiF, LiZnF and LiTiF samples, respectively. One can notice that the values of $M_s$ obtained and their variation are consistent with investigation results for substituted Li ferrites presented in [20, 22].

The typical behavior of TG and DTG curves during heating of ferrite sample in thermal analyzer is shown in Fig. 2. Clearly, if no chemical reactions that affect the change in mass of ferrite sample occur in a certain temperature range, then the TG curve remains unchanged without magnetic field (Fig. 2, dashed TG curve). The TG curve under magnetic field demonstrates the presence of mass gain
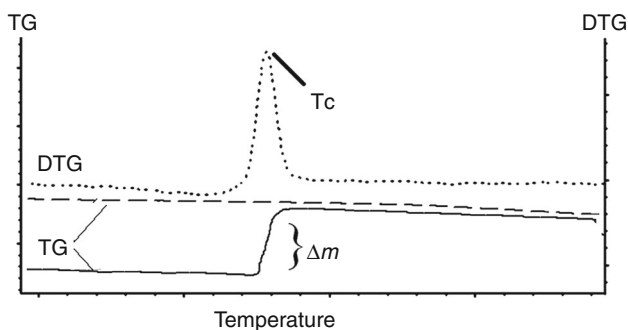
Fig. 2 TG and DTG curves for ferrite sample at thermogravimetric analysis in magnetic field (solid TG curve) and without magnetic field (dashed TG curve)

($\Delta m$) at temperature of ferrimagnet–paramagnet transition (Curie point) for ferrite phase presented in the sample (Fig. 2, solid TG curve). The DTG curve as the derivative TG curve under magnetic field allows determining more exactly the Curie temperature of this transition and hence to characterize the ferrite phase in the sample. Moreover, the number of peaks on the DTG curve corresponds to the number of ferrite phases dominating in the sample.

Figure 3 shows the TM analysis for LiF, LiZnF and LiTiF samples with 100% mass content. The mass gain is
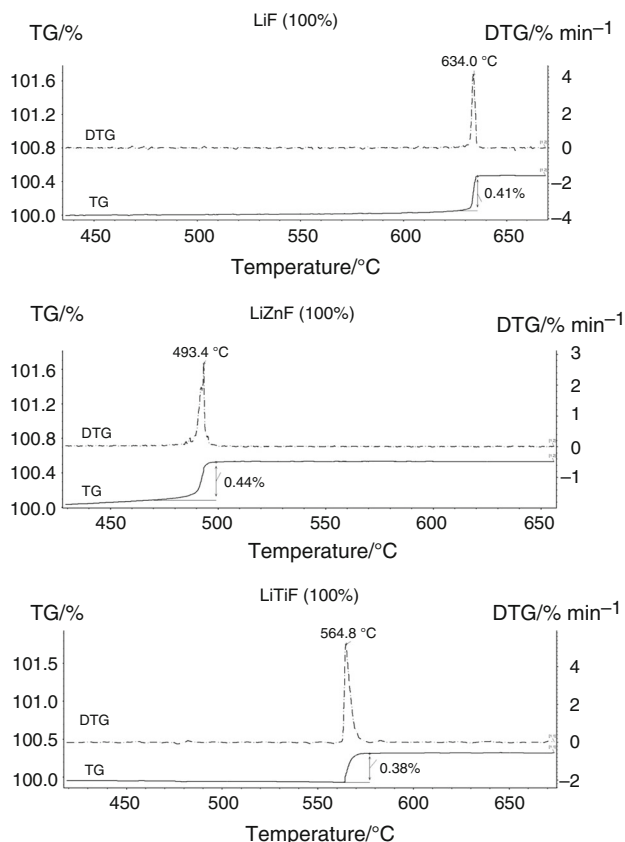


Fig. 3 TG and DTG curves obtained from thermomagnetometric analysis of lithium, lithium–zinc and lithium–titanium ferrites

observed on TG curves, and DTG curves show individual sharp peaks at temperatures corresponding to the Curie points in these ferrites. The values of Curie point are consistent with results obtained in [1].

As shown in Fig. 3, the lithium ferrite is characterized by the highest Curie temperature. By introducing zinc or titanium in lithium ferrite, a decrease in the Curie point is observed as a consequence of the diamagnetic substitution of iron cations by titanium or zinc ions occupying octahedral and tetrahedral positions in the cation sublattice, respectively [15]. According to the Néel theory, this diamagnetic substitution weakens the indirect exchange interaction of magnetic cations and causes the magnetization of domains in ferrimagnets to decrease [16].

As mentioned above, the introduction of additives in the lithium ferrite leads to a change in $M_s$. Thus, we should expect a change in $\Delta m$ of the ferrites with different $M_s$. Figure 3 shows that the LiZn ferrite exhibits the highest mass gain as compared to other ferrite samples. The variation in $\Delta m$ with saturation magnetization of ferrites is shown in Fig. 4. The error bars were estimated from a set of experimental data points obtained for several samples of the same composition. As can be seen, within the experimental error the magnitude of $\Delta m$ increases linearly with increasing magnetization of ferrite.

Using the obtained results of the mass gain at the Curie temperature for each ferrite, we constructed the calibration curves shown in Fig. 5 to estimate the concentration of ferrites in the composite mixture with various ferrite contents. It can be assumed that these curves have a linear form, since the variation in $\Delta m$ with $M_s$ shown in Fig. 4 is characterized by the linear behavior.

Then, the TM measurements of the samples consisting of ferrites mixed in various mass concentrations determined by the weighing on an analytical balance were
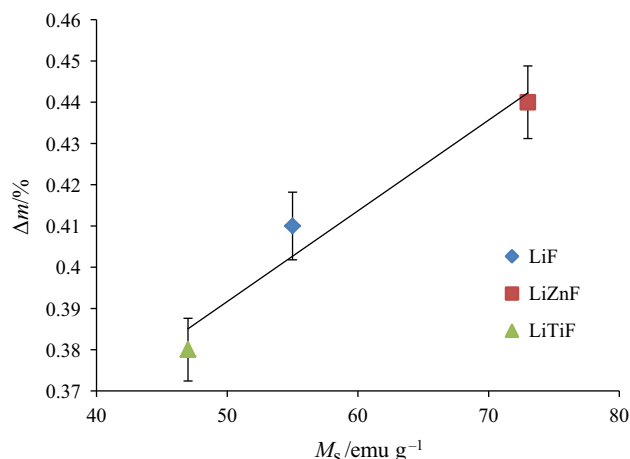


Fig. 4 Variation in ferrite mass gain at ferrimagnet–paramagnet transition with saturation magnetization of ferrites
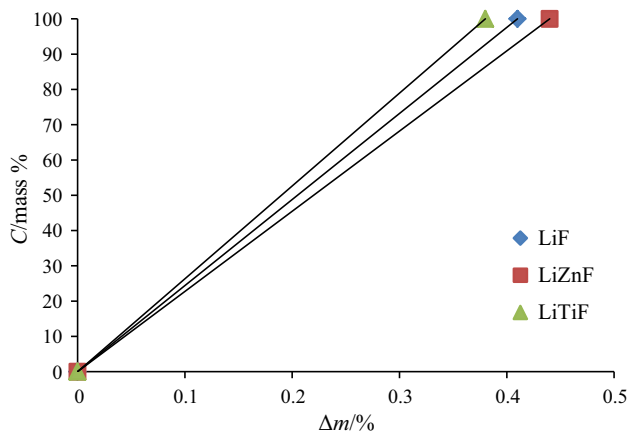
Fig. 5 Concentration of ferrites in the sample versus ferrite mass change at Curie point
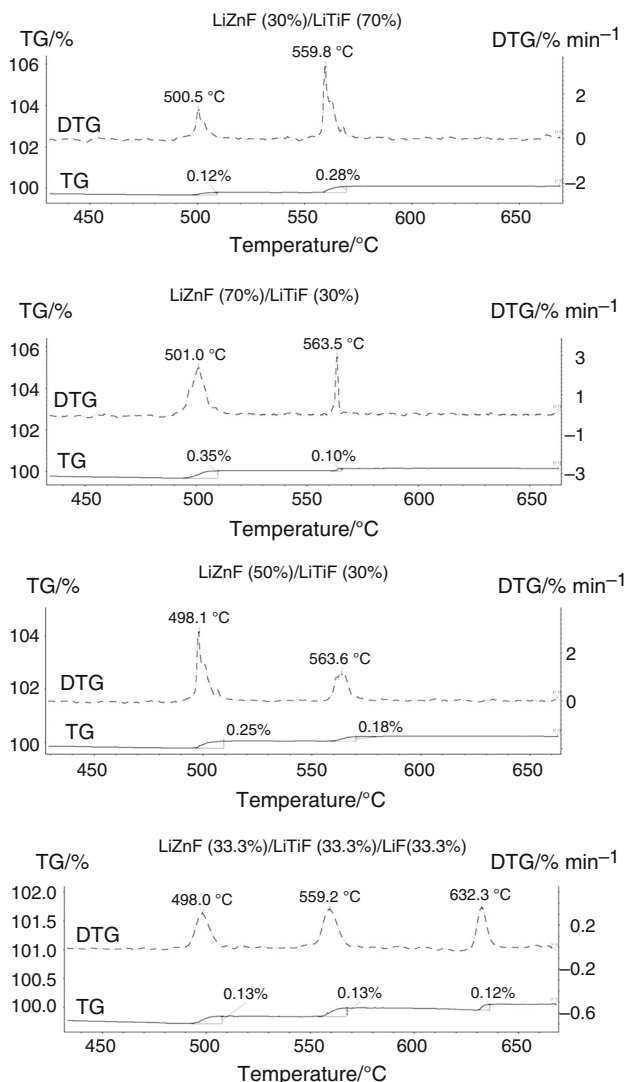
**Table 1** Result of the evaluation of concentrations

| Composition | Concentration by the weighing/mass % | Concentration by TM analysis/mass % |
|---|---|---|
| LiZnF | 30 | 27 |
| LiTiF | 70 | 73 |
| LiZnF | 70 | 73 |
| LiTiF | 30 | 27 |
| LiZnF | 50 | 53 |
| LiTiF | 50 | 47 |
| LiZnF | 33.3 | 32 |
| LiTiF | 33.3 | 36 |
| LIF | 33.3 | 32 |

taken. Figure 6 presents the TG and DTG curves for such samples. As can be seen, the sample consisting of several ferrite phases shows the number of mass gain on the TG curve, which corresponds to the number of phases presented in the sample. The magnitude of $\Delta m$ depends on the concentration of the ferrite with Curie point corresponding to the temperature of DTG peak.

According to the mass gain values for each sample shown in Fig. 6, the concentrations of ferrites presented in the samples were examined by the calibration curves. The results obtained are summarized in Table 1 and are compared with concentration values determined by the weighing on the analytical balance. It can be deduced that the experimental error in determining the phase concentration from obtained calibration curves is not more than 10%.

Therefore, using calibration curves obtained in advance for single-phase ferrites, it becomes possible to estimate the concentration of these ferrites in a composite sample consisting of several ferrite phases using TM analysis. However, it should be noted that a complex analysis using both of X-ray and TM analyses will be the most optimal in case of the formation of non-magnetic or weakly magnetic phase.

## Conclusions

In this work, the magneto-phase transitions in pure lithium, lithium–zinc and lithium–titanium ferrites with chemical compositions of $Li_{0.5}Fe_{2.5}O_4$, $Li_{0.4}Fe_{2.4}Zn_{0.2}O_4$ and $Li_{0.6}Fe_{2.2}Ti_{0.2}O_4$, respectively, were studied by thermomagnetometric analysis of the ferrite samples in magnetic field. The method of quantitative ferrite phase control based on the analysis of mass change of ferrite at Curie temperature was developed and tested using the composite samples with various ferrite concentrations. It can be concluded that the method proposed allows estimating the concentration



Fig. 6 TG and DTG curves for samples from ferrites mixed in various mass concentrations

of ferrite phases with the experimental error of not more than 10%.

# References

1. Surzhikov AP, Lysenko EN, Malyshev AV, Vlasov VA, Vasendina EA. Analysis of the phase composition and homogeneity of ferrite lithium-substituted powders by the thermomagnetometry method. J Therm Anal Calorim. 2013;112:739–45.

2. Astafyev AL, Lysenko EN, Surzhikov AP, Neudahina NA. Development of control method for ferrite phase composition using thermomagnetometric analysis. IOP Conf Ser Mater Sci Eng. 2014;66:012037.

3. Gallagher PK. Thermomagnetometry. J Therm Anal Calorim. 1997;49:33–44.

4. Warne SStJ, Gallagher PK. Thermomagnetometry. Thermochim Acta. 1987;110:269–79.

5. Lin DM, Wang HS, Lin ML, Lin MH, Wu YC. TG(M) and DTG(M) techniques and some of their applications on material study. J Therm Anal Calorim. 1999;58:347–53.

6. Sanders JP, Gallagher PK. Thermomagnetometric evidence of γ-Fe2O3 as an intermediate in the oxidation of magnetite. Thermochim Acta. 2003;406:241–3.

7. Norem SD, O'Neill MJ, Gray AP. The use of magnetic transitions in temperature calibration and performance evaluation of thermogravimetric systems. Thermochim Acta. 1970;1:29–38.

8. Wang T, Wang H, Wang F, Li J, Zhang Q, Huang X. Certification of reference materials of Alumel, nickel and iron for Curie point. J Therm Anal Calorim. 2018;131:1979–85.

9. Brown ME. Principles and practice. Gallagher PK, Series Editor. Handbook of thermal analysis and calorimetry, vol 1. Elsevier; 1998.

10. Weddle BJ, Robbins SA, Gallagher PK. Further studies on the use of simultaneous TM/DTA to establish magnetic transition temperatures. Pure Appl Chem. 1995;67:1843–7.

11. Luciani G, Costantini A, Branda F, Scardi P, Lanotte L. Thermal evolution of ferromagnetic metallic glasses. A study using TG(M) technique. J Therm Anal Calorim. 2003;72:105–11.

12. Opuchovic O, Niznansky D, Kareiva A. Thermoanalytical (TG/DSC/EVG-GC-MS) characterization of the lanthanide (Ho) iron garnet formation in sol-gel. J Therm Anal Calorim. 2017;130:1085–94.

13. Astafyev AL, Lysenko EN, Surzhikov AP. Estimation of thermomagnetometry method sensitivity for magnetic phase determination. IOP Conf Ser Mater Sci Eng. 2016;110:012090.

14. Cook W, Manley M. Raman characterization of & #x03B1;- and & #x03B2;-LiFe5O8 prepared through a solid-state reaction pathway. J Solid State Chem. 2010;183:322–6.

15. Smit J, Wijn HPJ. Ferrites. Physical properties of ferrimagnetic oxides in relation to their technical applications. Eindhoven: Philips Technical Library; 1959. p. 299.

16. Gorter EW. Saturation magnetization and crystal chemistry of ferrimagnetic oxides. J Philips Res Rep. 1954;9:295.

17. White GO, Patton CE. Magnetic properties of lithium ferrite microwave materials. Magn Magn Mater. 1978;9:299–317.

18. Patton CE, Edmondson CA, Liu YH. Magnetic properties of lithium zinc ferrite. J Appl Phys. 1982;53:2431–3.

19. Wilber WD, Kabos P, Patton CE. Brillouin light scattering determination of the spin-wave stiffness parameter in lithium-zinc ferrite. IEEE Trans Magn. 1983;19:1862–4.

20. Verma V, Gairola SP, Pandey V, Tawale JS, Su H, Kotanala RK. High permeability and low power loss of Ti and Zn substitution lithium ferrite in high frequency range. Magn Magn Mater. 2009;321:3808–12.

21. Widatallah HM, Ren XL, Al-Omari IA. The influence of TiO2 polymorph, mechanical milling and subsequent sintering on the formation of Ti-substituted spinel-related Li0.5Fe2.5O4. J Mater Sci. 2006;41:6333–8.

22. Sungshetti RM, Hiremath VA, Jali VM. Combustion synthesis and structural characterization of Li–Ti mixed nanoferrites. Bull Mater Sci. 2011;34:1027–31.